

TITLE PAGE

**Endothelial cell targeted deletion of PPAR $\gamma$  blocks rosiglitazone-induced plasma volume expansion and vascular remodeling in adipose tissue**

**Taro E. Akiyama, Graham E. Skelhorne-Gross, Elizabeth D. Lightbody, Rachel E. Rubino, Jia Yue Shi, Lesley A. McNamara, Neelam Sharma, Emanuel I. Zycband, Frank J. Gonzalez, Haiying Liu, John W. Woods, C. H. Chang, Joel P. Berger and Christopher J.B. Nicol.**

Cardiometabolic Disorders Department, Merck Research Laboratories, Kenilworth, NJ  
USA 07033 (TEA, LAM, NS, EIZ, HL, JWW, CHC, JPB)

Department of Pathology & Molecular Medicine, Queen's University, Kingston, Ontario,  
Canada K7L 3N6 (GESG, EDL, CJBN)

Cancer Biology & Genetics Division, Cancer Research Institute, Queen's University,  
Kingston, Ontario, Canada K7L 3N6 (RER, CJBN)

Department of Biomedical & Molecular Sciences, Queen's University, Kingston, Ontario,  
Canada K7L 3N6 (JYS, CJBN)

National Cancer Institute, National Institutes of Health, Bethesda, MD USA 20892 (FJG)

Takeda Pharmaceuticals International, Inc., 40 Landsdowne Street, Cambridge, MA,  
USA 02139 (JPB)

*JPET #250985*

RUNNING TITLE PAGE

**a) Running Title:**

Loss of endothelial cell-specific PPAR $\gamma$  blocks ROSI-induced edema

**b) Corresponding Author:**

*Christopher J. B. Nicol*

Queen's University Cancer Research Institute,

10 Stuart Street, Rm. 317

Kingston, ON, Canada K7L 3N6

Telephone: 613-533-6531

Fax: 613-533-6830

Email: [nicolc@queensu.ca](mailto:nicolc@queensu.ca)

**c) Manuscript Information:**

Number of text pages: 36

Number of tables: 0

Number of figures: 8

Number of references: 67

Abstract word count: 200

Introduction word count: 750

Discussion word count: 989

JPET #250985

**d) Non-Standard Abbreviations**

CYP11B2	Aldosterone synthase
ECF	Extracellular fluid
ECs	Endothelial cells
ENaC	Epithelial Na(+) channel
eWAT	Epididymal white adipose tissue
FAK	Focal adhesion kinase
HFD	High-fat diet
REMS	Risk evaluation and mitigation strategy
iWAT	Inguinal white adipose tissue
PPAR $\gamma$	Peroxisome proliferator-activated receptor $\gamma$
<i>Pparg</i> <sup>ff</sup>	<i>Pparg</i> -floxed wildtype control
<i>Pparg</i> <sup><math>\Delta</math>EC</sup>	<i>Pparg</i> EC-targeted knockout
PVE	Plasma volume expansion
qNMR	Quantitative nuclear magnetic resonance imaging
RAAS	Renin-angiotensin-aldosterone system
RBCs	Red blood cells
rWAT	Retroperitoneal white adipose tissue
TZD	Thiazolidinediones

**e) Recommended section assignment:**

Cellular and Molecular

## ABSTRACT

Thiazolidinediones (TZDs) are PPAR $\gamma$  agonists that represent an effective class of insulin sensitizing agents; however, clinical use is associated with weight gain and peripheral edema. To elucidate the role of PPAR $\gamma$  expression in endothelial cells (ECs) in these side effects, EC-targeted PPAR $\gamma$  knockout (*Pparg* <sup>$\Delta$ EC</sup>) mice were placed on high fat diet to promote PPAR $\gamma$  agonist-induced plasma volume expansion, and then treated with the TZD rosiglitazone. Compared to control *Pparg*<sup>f/f</sup> mice, *Pparg* <sup>$\Delta$ EC</sup> treated with rosiglitazone are resistant to an increase in extracellular fluid, water content in epididymal and inguinal white adipose tissue, and plasma volume expansion. Interestingly, histological assessment confirmed significant rosiglitazone-mediated capillary dilation within white adipose tissue of *Pparg*<sup>f/f</sup> mice, but not *Pparg* <sup>$\Delta$ EC</sup> mice. Analysis of ECs isolated from untreated mice in both strains suggests the involvement of changes in endothelial junction formation. Specifically, compared to cells from *Pparg*<sup>f/f</sup> mice, *Pparg* <sup>$\Delta$ EC</sup> cells have a 15-fold increase in focal adhesion kinase, critically important in EC focal adhesions, and >3-fold significant increase in vascular endothelial cadherin, the main component of focal adhesions. Together, these results indicate that rosiglitazone has direct effects on the endothelium via PPAR $\gamma$  activation, and point towards a critical role for PPAR $\gamma$  in ECs during rosiglitazone-mediated plasma volume expansion.

*JPET #250985*

## INTRODUCTION

Thiazolidinediones (TZDs), including marketed rosiglitazone (Avandia), are synthetic insulin sensitizing drugs that mediate their anti-diabetic effects through peroxisome proliferator-activated receptor (PPAR) $\gamma$ . TZDs also lower blood pressure and improve endothelial function (Parulkar et al., 2001; Haffner et al., 2002). Despite these beneficial effects, clinical use of TZDs (particularly in Europe) is limited by several adverse effects associated with their use (Gale, 2001). For instance, TZDs increase body weight gain in humans (2-3 kg for every percent decrease in HbA1c values), effects mainly attributed to increased subcutaneous fat depot size (Yki-Jarvinen, 2004). Since TZDs exert their insulin-sensitizing effects via PPAR $\gamma$  activation and given the well-established role of this receptor in promoting adipogenesis (Tontonoz et al., 1994; Spiegelman et al., 1997), such an effect is likely mechanism-based (Kliwer et al., 1992; Keller et al., 1993; Wahli et al., 1995; Kliwer et al., 2001; Berger and Moller, 2002; Wang et al., 2004; Ricote and Glass, 2007; Campbell et al., 2008).

TZDs also promote fluid retention or edema, which may partially contribute to increases in total body weight (Yki-Jarvinen, 2004). The incidence of edema is higher in patients treated with a combination of TZDs and insulin (Delea et al., 2003). In some cases, mild fluid retention can be treated by reducing the TZD dose and/or adding a diuretic (Hollenberg, 2003) although the majority of patients are not responsive to diuretic (Chen et al., 2005). TZD-induced edema may be receptor-mediated since structurally distinct, non-TZD PPAR $\gamma$  agonists also cause plasma volume expansion (PVE) in rodents (Berger et al., 2003). Likewise, the PPAR $\gamma$  Pro12Ala variant is a risk factor for PPAR $\gamma$  dual agonist-induced edema in Type 2 Diabetes (T2D) patients (Hansen et al., 2006). Importantly, body weight gain and edema are associated with increased risk for congestive heart failure (2.5 times greater) in patients receiving combination therapy that

JPET #250985

includes a TZD and insulin (Delea et al., 2003). However, the FDA lifted their restrictions on rosiglitazone after re-evaluation of the initial clinical trial data and continuous monitoring did not show heart infarct risks associated with the drug (Home et al., 2009; Food\_and\_Drug\_Administration, 2013; Food\_and\_Drug\_Administration, 2015). Given the pleiotropic beneficial effects of TZDs, it is crucial that the underlying mechanisms contributing to edema are elucidated.

Two independent groups showed targeted disruption of PPAR $\gamma$  in collecting ducts confers resistance to TZD-induced fluid retention and PVE in mice (Guan et al., 2005; Zhang et al., 2005). Transcriptional regulation by PPAR $\gamma$  of *Scnn1g*, the gene encoding the epithelial Na(+) channel (ENaC), reportedly plays a role in TZD-induced fluid retention by regulating renal salt absorption ((Pavlov et al., 2009; Beltowski et al., 2013). Another group reported that increased TZD-induced fluid retention is independent of ENaC (Vallon et al., 2009). Beyond fluid retention, PPAR $\gamma$  agonist-induced edema may be multifactorial in nature, including altered endothelial permeability (Walker et al., 1999; Wagner et al., 2012), sympathetic nervous system activity (Yoshimoto et al., 1997), interstitial ion transport (Hosokawa et al., 1999) and PPAR $\gamma$ -mediated expression of vascular permeability growth factor (Nesto et al., 2004). Nevertheless, more work is needed to elucidate the mechanism(s) involved.

The vasculature represents a potential 'target tissue' for TZD-mediated edema since it serves as a direct interface between circulating blood and interstitium, and expression of PPAR $\gamma$  was demonstrated in human endothelial cells (ECs) (Marx et al., 1999; Willson et al., 2001). Indeed, several PPAR $\gamma$  direct and indirect target genes were identified in ECs, encoding proteins relevant to blood pressure regulation and EC permeability such as NO production, chemotaxis, apoptosis and redox signaling (Marx et al., 1999). Focal adhesions between ECs are maintained

JPET #250985

by focal adhesion kinase (FAK), which normally regulates EC matrix attachment (Romer et al., 2006). FAK normally maintains endothelial adherens junctions, while FAK deletion in mouse ECs disrupts their function and leads to edema (Schmidt et al., 2013). PPAR $\gamma$  agonists decrease FAK expression (Chen et al., 2005) suggesting PPAR $\gamma$  may play a critical role in weakening EC junctions, and their major component VE-cadherin (Mehta and Malik, 2006).

To directly examine the hypothesis that EC-expressed PPAR $\gamma$  plays a role in mediating TZD-induced edema *in vivo*, studies were performed using mice with targeted disruption of PPAR $\gamma$  in EC (*Pparg* <sup>$\Delta$ EC</sup>) (Nicol et al., 2005). Here we present the first evidence that *Pparg* <sup>$\Delta$ EC</sup> mice, versus control floxed (*Pparg*<sup>ff</sup>) littermates, are refractory to rosiglitazone-mediated increases in extracellular fluid levels and PVE. Further, both FAK and VE-cadherin are increased among ECs isolated from *Pparg* <sup>$\Delta$ EC</sup> versus controls. These results suggest a critical role for EC-expressed PPAR $\gamma$  in mediating TZD-induced edema, which may help human patients treated with these drugs.

*JPET #250985*

## MATERIALS AND METHODS

### Animals

All mice studies were in accordance with protocols approved by the Animal Use and Care Committees of Merck and Queen's University, and conform with the U.S. National Institutes of Health Guide for the Care and Use of Laboratory Animals and the Canadian Council on Animal Care Guidelines. Mice were housed in cages on a 12-h light/dark cycle, with food and water provided ad libitum. Mouse models of endothelial cell targeted PPAR $\gamma$  deletion (*Pparg* <sup>$\Delta$ EC</sup> mice) were generated by crossing our *Pparg*<sup>ff</sup> mice (Akiyama et al., 2002) with Tie2-Cre<sup>+</sup> transgenic mice (Kisanuki et al., 2001) as previously described and characterized (Nicol et al., 2005; Kanda et al., 2009). Mice were genotyped using polymerase chain reaction as previously reported (Nicol et al., 2005). Littermates homozygous for the floxed PPAR $\gamma$  gene, but lacking Cre expression, were used as controls. We previously reported characterization of both male and female *Pparg*<sup>ff</sup> or *Pparg* <sup>$\Delta$ EC</sup> mice, with very few differences identified, and none of which pertained to ability to respond to a TZD (Nicol et al., 2005). In fact, the only notable sex difference observed was significantly increased heart rate levels among salt-loaded PPAR $\gamma$  <sup>$\Delta$ EC</sup> KO males compared similarly treated PPAR $\gamma$ <sup>ff</sup> WT males, which also trended in that direction for female mice. In light of this, and pilot studies showing male mice recapitulated the effects of TZDs on fluid retention, we therefore surmised that male mice would serve as a good model for TZD-induced edema in humans (that occurs to same extent in both sexes). At 6 weeks of age, male mice were placed on a HFD (RD12492- 60 kcal% fat, 20 kcal% carbohydrate and 20 kcal% protein, Research Diets, New Brunswick, NJ) for 12 weeks.

### Rosiglitazone treatment



*JPET #250985*

Rosiglitazone was incorporated into the diet (Research Diets, D12492) at a level of 100 mg/kg diet. Mice were fed rosiglitazone-formulated or vehicle control diet for a period of 14 days ad libitum.

### **Plasma glucose and insulin measurements**

Blood taken from tail vein was collected in heparinized capillary tubes (Clay Adams SurePrep heparinized capillary tubes, Becton Dickinson and Co., Sparks, MD) and centrifuged at 11,500 x g for 10 minutes to separate plasma. Plasma glucose (Autokit Glucose, Wako Diagnostics, Richmond VA) and insulin levels (Ultrasensitive rat insulin ELISA, ALPCO diagnostics, Sweden) were determined according to protocols provided with the kits.

### **Bioelectrical impedance analysis for determination of extracellular fluid volume**

Twenty-four hours following the final dose, mice were anesthetized with ketamine (85 mg/kg, i.m.) and xylazine (10 mg/kg, i.m.). Animals were positioned on a non-conductive surface in dorso-lateral recumbency and extracellular fluid volume was determined by bioelectrical impedance analysis, following procedures described by the manufacturer (Hydra ECF/ICF Impedance Analyzer Model 4, Xitron, San Diego, CA, USA) and by B. H. Cornish and colleagues (Quirk et al., 1997). A tetrapolar impedance monitor was used to measure impedance, and hence the total body water, over a frequency range of 5 kHz to 1 MHz. Source electrodes (1 cm x 26G stainless steel needles) were inserted 5 mm subcutaneously. Detector electrodes were inserted along the midline at the anterior point of the sternum and the anterior point of the penis. The distance between electrodes was measured and included for data modeling.

JPET #250985

### **Plasma volume measurement**

After determination of extracellular fluid volume, plasma volume was measured in anesthetized animals using a dye dilution technique following methods described previously (Belcher and Harriss, 1957), with minor modifications. Evans blue dye solution (25 mg/ml in physiological saline) was filtered through a 0.22  $\mu\text{m}$  filter prior to injection into a jugular vein. Twenty minutes after injection, a heparinized blood sample (2 ml) was withdrawn from the descending aorta. Plasma was separated by centrifugation of the blood at 1,100 x g for 15 min.; samples were kept at  $-80^{\circ}\text{C}$  until assayed. Absorbance of the thawed plasma was read at 620 nm, and plasma Evans blue dye concentrations were calculated according to a standard curve generated by a serial dilution of the 25 mg/ml Evans blue dye-saline solution. Plasma volume was calculated by using the dilution factors of Evans blue as shown below.

$$\text{Plasma volume} = \frac{[\text{dye}] \text{ injected} \times \text{volume of dye injected}}{[\text{dye}] \text{ in plasma}}$$

### **Tissue water content measurement**

Immediately after euthanasia, epididymal fat pad, pararenal fat pad, inguinal fat pad, and gastrocnemius muscle were removed and weighed, and placed in individual glass scintillation vials. Weighed tissues were subjected to a vacuum-applied Speed Vac centrifugation/drying process over a 24-hours period. After this drying process, tissues were weighed again to calculate individual tissue water content.

### **Quantitation of enlarged capillaries in white adipose tissue**

*JPET #250985*

At necropsy, adipose tissue was collected from epididymal and inguinal depots. Samples of white adipose tissue weighing approximately 1 gm were fixed by immersion in several changes of 2% freshly prepared paraformaldehyde (in 0.1 M phosphate buffer pH 7.3) for 48 hrs at 4°C. Following fixation the tissue was dehydrated through graded ethanol, exchanged into xylene and embedded in paraffin using a Leica TP1026 embedding system. Paraffin sections (8µm) were subsequently cut on a Leica RM2155 microtome, transferred to glass slides and stained with hematoxylin and eosin. The number of enlarged capillaries on each slide was quantitated in a blinded fashion as follows: each section was first examined on a Zeiss Axioplan 2 microscope equipped with a digital stage using a 5x objective and a red filter, to preclude bias from observing red blood cells (RBCs), that still allowed easy visualization of the tissue. Using the digital stage controls, 10 widely separated locations scattered across the section were marked. This marking ensured that tissue was present and cells at each location were well preserved adipocytes free of mechanical defects, and not large blood vessels, lymph nodes or connective tissue. After marking 10 locations, each were then re-examined in detail under white light illumination using a 40x objective. Once the stage was relocated to the marked locations, the stage was not moved in the x-y plane although focus was adjusted as needed. The number of enlarged capillaries observed in each 40x field were then recorded. For counts, enlarged capillaries were defined as any capillary containing a cluster of 3 or more RBCs in each of the 10 sections. Capillaries in which the RBCs lined up in a single file were most likely of normal size and were not counted as enlarged.

### **Immunofluorescent Staining**

JPET #250985

Formalin fixed, paraffin-embedded (FFPE) lung tissue blocks from (n=3) untreated *Pparg*<sup>ff</sup> and *Pparg*<sup>ΔEC</sup> mice were sectioned into 5 μm slices, mounted on slides, and incubated at 55°C overnight. Samples were deparaffinized and rehydrated by washing in: xylene, 4 min; xylene, 4 min; xylene, 4 min; 100% ethanol, briefly; 85% ethanol, briefly; 70% ethanol, briefly; ddH<sub>2</sub>O, 4 min. Slides were placed in 1:10 sodium citrate buffer solution at 95°C for 20 min, then trypsinized with 1× trypsin (Sigma) for 20 min at 37°C. After washing, the slides were placed in Triton X/TBS buffer solution, followed by a 30 min incubation period in 5% BSA block in TBS. After washing, primary antibody for VE-Cadherin (Enzo Life Sciences, ALX-803-305-C100; 1:200) was applied in a 5% BSA solution for 3.5 hours at room temperature. Slides were rinsed with Tris-buffered saline (TBS), and then incubated in fluorescein isothiocyanate (Santa Cruz; 1:500) and Alexa Fluor 594 (Invitrogen; 1:500) fluorescent-conjugated secondary antibodies in 5% BSA for 15 min at room temperature. After a final rinsing regimen, tissues were coverslipped with mounting media containing 4', 6-diamidino-2-phenylindole (DAPI) stain (Vectashield). Fluorescence was detected and quantitated using a Quorum WaveFX-X1 spinning disk confocal system (Quorum Technologies Inc., Guelph On., Canada) and MetaMorph Offline (64-bit; Version 7.7.0.0).

### **Endothelial Cell Isolation**

Endothelial cells (ECs) were isolated from lung samples collected from (n=3) untreated *Pparg*<sup>ff</sup> and *Pparg*<sup>ΔEC</sup> mice according to an established protocol (Kobayashi et al., 2005). Briefly, lungs were collected at necropsy, minced finely and digested with Collagenase A and washed repeatedly. ECs were selected using dynabeads (Life Technologies Inc., Burlington On, Canada) conjugated to PECAM-1 antibody (Santa Cruz Biotechnology, Inc., San Diego, CA)

*JPET #250985*

following manufacturer's instructions. The dynabeads were washed 4x with 4ml of 10% FBS in DMEM to ensure purity of the EC population, and then trypsinized to remove the cells from the beads. Total RNA was collected immediately following cell isolation according to the TRIZOL method. Briefly, cells were suspended in TRIZOL (Invitrogen, Carlsbad, CA) for 5 min then chloroform was added for 3 min. After centrifugation, RNA was extracted from the aqueous layer using isopropanol, 10 min; 75% ethanol, 5 min and resuspended in RNase-free water.

### **Quantitative Real-time Polymerase Chain Reaction Assay**

Following UV-spectrophotometric analyses ( $A_{260/280}$ ) to determine purity and concentrations, RNA samples were converted to cDNA using the iScript cDNA synthesis kit (Bio-Rad). cDNA concentrations were quantified as described for RNA above, and combined with iQ SYBR Green mix (BioRad, Hercules, CA), autoclaved commercially-available ddH<sub>2</sub>O and PrimePCR Assay primers (cat#10025636, BioRad, Hercules, CA) to evaluate FAK (PTK2) expression levels. Assays were performed on an iQ5 Multicolor Real-Time PCR Detection System (Bio-Rad, Hercules, CA) thermocycler programmed with the following conditions: 5 min 95°C hot-start, followed by 50 cycles of 95°C for 15 s, 65°C for 15 s and 72°C for 30 s.

### **Statistical analysis**

All values are presented as means +/- standard error. Statistical analyses were performed using GraphPad Prism 6 software. Multiple group comparisons were assessed using a two-way ANOVA followed by bonferroni post-hoc tests, with a p value <0.05 considered statistically significant.

## RESULTS

### ***Pparg*<sup>ΔEC</sup> mice are healthy, viable and able to gain weight normally on a HFD**

*Pparg*<sup>ΔEC</sup> mice are viable, appear healthy and exhibit no gross abnormalities. After 12 weeks on a HFD, *Pparg*<sup>ΔEC</sup> mice did not differ from *Pparg*<sup>f/f</sup> control littermates in terms of body weight (*Pparg*<sup>ΔEC</sup> mice 41.4 +/- 0.9 g versus *PPARγ*<sup>WT</sup> 42.7 +/- 0.9 g) or food intake (*Pparg*<sup>ΔEC</sup> 17.9 +/- 0.4 kcal/day versus *Pparg*<sup>f/f</sup> 17.6 +/- 0.5 kcal/day, based on RD12492 diet). Baseline lean, fat and fluid mass in *Pparg*<sup>ΔEC</sup> mice were also similar to *Pparg*<sup>f/f</sup> controls as measured by quantitative NMR (Fig. 1). Others have reported an attenuation in rosiglitazone-induced body weight gain in collecting duct-specific *PPARγ* null mice versus control mice presumably due, in part, to reduced fluid retention (Guan et al., 2005). In this study, there was a tendency for rosiglitazone-treated *Pparg*<sup>f/f</sup> mice to gain weight relative to corresponding vehicle-treated mice, however, this trend was not statistically significant (Supplemental Fig. 1). This apparent discrepancy in results likely reflects the difference in the baseline body weights of the mice prior to treatment (~42g in this study vs. ~29g in Guan, Y et al. 2005) since rosiglitazone is more likely to promote weight gain in leaner mice.

### **EC-expressed *PPARγ* is not required for TZD-mediated anti-diabetic efficacy**

Prior to rosiglitazone treatment, the baseline levels of ambient plasma glucose and insulin were unchanged in *Pparg*<sup>ΔEC</sup> mice relative to *Pparg*<sup>f/f</sup> mice on a HFD (Fig. 2A,B). Rosiglitazone treatment of *Pparg*<sup>f/f</sup> mice resulted in a dramatic reduction in plasma insulin, but not glucose levels (Fig. 2A,B), consistent with the results of other studies in C57B6 mice treated with TZDs (Gensch et al., 2007; Liu et al., 2007). In *Pparg*<sup>ΔEC</sup> mice, rosiglitazone also normalized plasma insulin levels to a similar extent as in *Pparg*<sup>f/f</sup> with no effect on glucose levels (Fig. 2A,B),

JPET #250985

suggesting that EC-expressed PPAR $\gamma$  is not required for TZD-mediated improvement in insulin sensitivity.

A histological analysis of epididymal and inguinal white adipose tissue (eWAT and iWAT) depots in control mice treated with rosiglitazone revealed the presence of pockets of smaller, more multilocular adipocytes (Fig. 3A,B). Such changes are consistent with a more 'activated' adipocyte phenotype in response to PPAR $\gamma$  agonism and have been described in other rodent models (Okuno et al., 1998; de Souza et al., 2001). Similar changes in the size and arrangement of adipocytes were also observed in eWAT and iWAT of *Pparg* <sup>$\Delta$ EC</sup> mice treated with rosiglitazone (Fig. 3C,D). No significant differences were observed in tissue weights assessed (Supplemental Fig. 1). It was suggested that a TZD-induced shift towards smaller adipocytes improves insulin resistance by decreasing the proportion of larger adipocytes that secrete elevated levels of free fatty acids (Okuno et al., 1998). Consistent with this notion, the appearance of multilocular adipocytes coincides with similar insulin lowering in both *Pparg* <sup>$\Delta$ EC</sup> and *Pparg*<sup>ff</sup> mice upon rosiglitazone treatment. In addition, the presence of multilocular adipocytes in rosiglitazone-treated *Pparg* <sup>$\Delta$ EC</sup> may serve as an internal control demonstrating that PPAR $\gamma$  expression in adipocytes is unaffected by EC-targeted disruption of PPAR $\gamma$ .

### **EC-expressed PPAR $\gamma$ plays a critical role for TZD-induced capillary vasodilation**

The hypotensive effects of TZDs in humans and preclinical species are well documented (Pershad Singh et al., 1993; Buchanan et al., 1995; Ogihara et al., 1995; Walker et al., 1999). Though the mechanism(s) for TZD-induced blood pressure lowering are not entirely clear, a reduction in total peripheral resistance may be an important component of this response since TZDs cause significant capillary vasodilation in preclinical species (Buchanan et al., 1995;

JPET #250985

Kotchen et al., 1996; Ghazzi et al., 1997; Song et al., 1997; Kawasaki et al., 1998). PPAR $\gamma$  activation with TZDs also decreases the pressure-induced platelet aggregation that leads to hypertension (Rao et al., 2014). Hypertension is also driven by the renin-angiotensin-aldosterone system (RAAS), and multiple groups have shown that PPAR $\gamma$  ligands reduce blood pressure by inhibiting the RAAS (Sugawara et al., 2012). Multiple PPAR $\gamma$  ligands decrease mRNA expression of the angiotensin II type 1 receptor expression (Sugawara et al., 2001). Additionally, PPAR $\gamma$  agonists inhibit angiotensin induced aldosterone production/secretion by suppressing aldosterone synthase (CYP11B2) (Urano et al., 2011). In one study using human subjects, it was concluded that rosiglitazone does not affect vasodilation (Rennings et al., 2006), however, this finding is not supported by the majority of the literature.

In the current study, *Pparg*<sup>f/f</sup> mice treated with rosiglitazone exhibited a clear increase in the number of enlarged capillaries in both eWAT and iWAT depots versus vehicle treatment (Fig. 4A,B). Strikingly though, the effects of rosiglitazone on capillary vasodilation (Fig. 3C,D) in white adipose tissue depots of control mice were noticeably absent in *Pparg* <sup>$\Delta$ EC</sup> mice. Interestingly, these vascular effects of rosiglitazone appear to be tissue-specific since rosiglitazone treatment did not affect capillary vasodilation within skeletal muscle tissue (not shown). The lack of rosiglitazone-induced capillary expansion in the white adipose tissue of *Pparg* <sup>$\Delta$ EC</sup> mice may also help to explain the resistance to TZD-induced blood pressure lowering shown previously in the same mouse model (Nicol et al., 2005). Together, these results indicate that EC-expressed PPAR $\gamma$  is necessary for mediating the vasodilatory effects of rosiglitazone in adipose tissue and may provide mechanistic insight into blood pressure regulation by TZDs.



## EC PPAR $\gamma$ plays a critical role in TZD-induced extracellular fluid and plasma volume expansion

To address whether the observed vascular changes in WAT following rosiglitazone treatment could ultimately impact systemic fluid dynamics, the effect of rosiglitazone on multiple surrogate markers of fluid accumulation was examined in *Pparg* <sup>$\Delta$ EC</sup> mice. First, the results of quantitative nuclear magnetic resonance imaging (qNMR) measurement show that while the EC-targeted deletion of PPAR $\gamma$  did not affect whole-body fluid mass, rosiglitazone induction of total fluid mass in control mice was attenuated in *Pparg* <sup>$\Delta$ EC</sup> mice (Fig. 5A).

Next, bioelectrical impedance, a term used to describe the response of a living organism to an externally applied electric current, was examined in both vehicle and rosiglitazone-treated *Pparg* <sup>$\Delta$ EC</sup> and *Pparg*<sup>ff</sup> mice. Measurement of the opposition to the flow of that electric current through the tissues has proven useful as a non-invasive method for quantifying extracellular fluid (ECF) (Quirk et al., 1997). Our results show that while basal levels of ECF are not significantly different in vehicle-treated *Pparg* <sup>$\Delta$ EC</sup> mice versus *Pparg*<sup>ff</sup> controls, while *Pparg* <sup>$\Delta$ EC</sup> mice are almost completely resistant to rosiglitazone induction of ECF observed in PPAR $\gamma$ <sup>WTs</sup> (Fig. 5B).

The Evans blue technique is widely used to determine plasma volume in human, dog and rat (Merrill and Cowley, 1987; Iwasaki et al., 2004; Ross and Idah, 2004). Using this technique, *Pparg* <sup>$\Delta$ EC</sup> mice have normal plasma volume levels that are not significantly different from control mice (Fig. 5C). However, the response to rosiglitazone was markedly attenuated compared to *Pparg*<sup>ff</sup> mice where a significant elevation in plasma volume was observed (Fig. 5C). Taken together, these data indicate that EC PPAR $\gamma$  plays a central role in regulating plasma volume and ECF following TZD treatment.

JPET #250985

## ***Pparg*<sup>ΔEC</sup> mice are resistant to rosiglitazone-induced fluid accumulation in white adipose tissue**

Following rosiglitazone treatment, tissue biopsies were collected from epididymal, inguinal, and retroperitoneal white adipose tissue (eWAT, iWAT and rWAT, respectively) and skeletal muscle. Tissue weights were recorded prior to and after lyophilization of the tissue biopsies and normalized to baseline 'wet' tissue weights to determine tissue water content. Rosiglitazone-treated control mice exhibit markedly increased water content in each of the WAT depots examined, but not in skeletal muscle (Fig. 6). On the other hand, water content in both skeletal muscle and white adipose tissue remains unchanged in rosiglitazone-treated *Pparg*<sup>ΔEC</sup> mice versus vehicle-treated controls (Fig. 6). Notably, the appearance of capillary vasodilation and elevated tissue water content coincides in terms of tissue specificity (white adipose tissue but not skeletal muscle). Based on this, the possibility exists that arterial fluid more readily crosses the endothelium of enlarged capillaries within white adipose tissue, though capillary permeability was not specifically examined in this study. The combined data imply that TZD-induced fluid accumulation occurs in a tissue-specific manner and requires a functional PPAR $\gamma$  receptor in ECs.

## **PPAR $\gamma$ deficiency in ECs leads to alterations in endothelial cell junctions**

*Fak* mRNA expression was measured in lung endothelial cells isolated from *Pparg*<sup>ΔEC</sup> and *Pparg*<sup>f/f</sup> mice. Lung tissue was chosen here due to its high proportion of endothelial cells. Relative to *Pparg*<sup>f/f</sup> mice, *Pparg*<sup>ΔEC</sup> mice expressed less than 0.04% *Pparg* mRNA, normalized to *Gapdh* mRNA, in their ECs (p=0.055) (Fig. 7A). Despite not being statistically significant, this difference is likely biologically significant and is consistent with our previous data

JPET #250985

demonstrating PPAR $\gamma$  within ECs is disrupted in our mouse model (Nicol et al., 2005). Additionally, *Fak* mRNA expression, normalized to *Gapdh* mRNA, was 15-fold higher in *Pparg* <sup>$\Delta$ EC</sup> ECs versus controls (p=0.06) (Fig. 7B). Importantly, this result is consistent with other reports that PPAR $\gamma$  negatively regulates FAK expression (Chen et al., 2005) which may explain the increased sensitivity to TZD-induced edema observed in *Pparg*<sup>ff</sup> mice treated with rosiglitazone.

Given the increase in *Fak* expression, immunofluorescence was used to evaluate EC junctions. FFPE lung samples from (n=3) *Pparg* <sup>$\Delta$ EC</sup> and *Pparg*<sup>ff</sup> mice were cut and stained with PECAM and VE-Cadherin to respectively identify EC populations and junctions. VE-Cadherin expression quantified in PECAM<sup>+</sup> cells is significantly >3-fold higher in *Pparg* <sup>$\Delta$ EC</sup> samples versus *Pparg*<sup>ff</sup> controls (p<0.05) (Fig. 7C-E).

JPET #250985

## DISCUSSION

PPAR $\gamma$  agonists have potent cardiovascular effects including capillary vasodilation, mean arterial blood pressure lowering and plasma volume expansion (PVE). However, the precise mechanisms by which these effects occur is not entirely clear and may be multifactorial. The results of multiple studies, including both pharmacologic and genetic, suggest that fluid retention mediated by PPAR $\gamma$  in the collecting duct is an important factor that contributes to the development of TZD-induced edema. In addition to the kidney, PPAR $\gamma$  is well-expressed in ECs. This study was undertaken with the goal of better understanding what role, if any, PPAR $\gamma$  in the endothelium plays in TZD-induced edema. The side-effects of TZDs observed in humans, including PVE, hemodilution, edema, increased adiposity and weight gain are recapitulated in rodent species (Berger and Moller, 2002); thus, preclinical rodent models are useful to help define the *in vivo* mechanisms causing these effects. Toward this end, *Pparg* <sup>$\Delta$ EC</sup> mice were, placed on a HFD (a condition that promotes PPAR $\gamma$  agonist induced PVE) and treated with a prototypical TZD, rosiglitazone.

Our results show that *Pparg* <sup>$\Delta$ EC</sup> mice have similar total body weight gain as well as lean, fat and fluid mass relative to control littermates on HFD, and no significant changes in body or tissue weights following rosiglitazone treatment. *Pparg* <sup>$\Delta$ EC</sup> mice also remain responsive to the insulin-lowering effects of rosiglitazone, suggesting that PPAR $\gamma$  in ECs is not critical to overall metabolic phenotype (at least related to diabetes and obesity) under ambient conditions. In response to rosiglitazone treatment, however, a number of interesting phenotypes emerged in the *Pparg* <sup>$\Delta$ EC</sup> mice that have relevance both to the regulation of blood pressure and development of edema. With regard to the former, the results of histological analysis indicate that *Pparg* <sup>$\Delta$ EC</sup> mice are refractory to the capillary vasodilatory effects of rosiglitazone in multiple white adipose

JPET #250985

depots. In addition, rosiglitazone also reduced adipocyte size, an effect that is consistent with previous findings showing that a TZD agonist of PPAR $\gamma$  increased the number of small adipocytes without a change of white adipose tissue mass in obese Zucker rats (Okuno et al., 1998). Based on these observations, one might therefore expect that TZDs do not significantly reduce total peripheral resistance and blood pressure in *Pparg* <sup>$\Delta$ EC</sup> mice unless under diabetic conditions, in agreement with a previous report (Nicol et al., 2005). Histological analysis also revealed that rosiglitazone-induced capillary vasodilation occurs in a tissue-specific manner (white adipose but not in skeletal muscle). It is tempting to speculate that paracrine effects originating from adipocytes, where PPAR $\gamma$  is highly expressed, contribute to vascular remodeling in adipose tissue, a possibility that requires future investigation for example by using adipocyte targeted PPAR $\gamma$  KO mice. An obvious implication of our histological observations is that TZD-induced capillary vasodilation leads to increased capillary permeability and the development of edema.

Concerns over the potential for TZDs to promote the risk of myocardial infarction (Nissen and Wolski, 2007; Kung and Henry, 2012) prompted the FDA to require black box labels warnings on Avandia in 2007 (Starner et al., 2008). However, the FDA lifted restrictions in 2013 after re-evaluating the 2009 RECORD clinical trial (a six-year, open label randomized control trial), which did not show heart infarct risks associated with the drug (Home et al., 2009; Food\_and\_Drug\_Administration, 2013). In 2015, the FDA further removed the Risk Evaluation and Mitigation Strategy (REMS) requirements for rosiglitazone-containing medicines after continuous monitoring indicated no new pertinent safety information (Food\_and\_Drug\_Administration, 2015). Collectively, our data is the first to show that normal PPAR $\gamma$  expression suppresses EC-specific FAK expression, which in turn, regulates EC

JPET #250985

junctions and vascular permeability. This suggests a mechanistic link that may explain the rosiglitazone-induced edema demonstrated by *Pparg*<sup>ff</sup> but not *Pparg*<sup>ΔEC</sup> mice (Fig. 8A,B). By negatively regulating FAK, PPAR $\gamma$  in ECs may cause the destabilization of EC junctions. This is further suggested by the reduction of VE-Cadherin in lung EC junctions in *Pparg*<sup>ff</sup> compared to *Pparg*<sup>ΔEC</sup> mice. Indeed, a consensus statement from the American Heart Association and American Diabetes Association posited that TZDs may interact synergistically with insulin to cause arterial vasodilatation, leading to sodium reabsorption with a subsequent increase in extracellular volume, thereby resulting in peripheral edema in humans (Nesto et al., 2004). It is also suggested that the combination of decreased total peripheral resistance and expanded plasma volume is sufficient to cause an increase in interstitial fluid retention (Chen et al., 2005). Rosiglitazone-induced arterial vasodilation was accompanied by increased total body fluid mass as determined by qNMR, increased ECF, elevated tissue water content in white adipose tissue as well as plasma volume expansion in *Pparg*<sup>ff</sup> but not *Pparg*<sup>ΔEC</sup> mice suggesting a direct PPAR $\gamma$ -dependent effect.

In summary, this study shows that plasma volume expansion and increased extracellular fluid volume (i.e. edema) is mediated by rosiglitazone acting directly on receptors present in the vascular endothelium. The combined effects of a PPAR $\gamma$  agonist on both renal and vascular PPAR $\gamma$  thus appear to contribute to the induction of edema. Given that both rosiglitazone and pioglitazone are known to cause PPAR $\gamma$ -induced edema, the results of this study are likely broadly applicable to both rosiglitazone and pioglitazone treatment of human T2D patients. The involvement of PPAR $\gamma$  expressed in the hematopoietic system cannot be ruled out as a confounder in mediating the effects of rosiglitazone, since Tie2 expression is reported in multiple hematopoietic cell types including B cells and T cells (Constien et al., 2001). Modulation of

*JPET #250985*

inflammatory signaling may influence factors such as capillary permeability and vascular tone, and remains to be investigated.

From a therapeutic standpoint, the identification of selective modulators of PPAR $\gamma$  that maintain robust anti-diabetic efficacy with reduced PVE in rodents suggests that these novel ligands may have effects on ECs that are distinct from those of TZDs and other full agonists of PPAR $\gamma$ . Further studies that focus on PPAR $\gamma$  activity in ECs and kidney should help to clarify the mechanisms responsible for the improved therapeutic window of selective modulators of PPAR $\gamma$  in preclinical species, and may lead to the identification of potential biomarkers of PPAR $\gamma$  agonist-induced edema.

JPET #250985

## ACKNOWLEDGMENTS

The authors would like to acknowledge Sarah Nersesian from Designs that Cell for illustrations (<https://designsthatcell.wixsite.com/home>). There are no conflicts of interest to declare.

## AUTHOR CONTRIBUTIONS

*Participated in research design:* Akiyama, Skelhorne-Gross, Gonzalez, Berger and Nicol.

*Conducted experiments:* Akiyama, Skelhorne-Gross, Lightbody, Rubino, Shi, McNamara, Sharma, Zycband, Liu, Woods, Chang and Nicol.

*Contributed new reagents or analytic tools:* Gonzalez and Nicol.

*Performed data analysis:* Akiyama, Skelhorne-Gross, Lightbody, Rubino, Shi, McNamara, Sharma, Zycband, Liu, Woods and Chang.

*Wrote or contributed to the writing of the manuscript:* Akiyama, Skelhorne-Gross, Lightbody, Gonzalez, Berger and Nicol.



JPET #250985

## REFERENCES

- Akiyama TE, Sakai S, Lambert G, Nicol CJ, Matsusue K, Pimprale S, Lee YH, Ricote M, Glass CK, Brewer HB, Jr. and Gonzalez FJ (2002) Conditional disruption of the peroxisome proliferator-activated receptor gamma gene in mice results in lowered expression of ABCA1, ABCG1, and apoE in macrophages and reduced cholesterol efflux. *Molecular and cellular biology* **22**:2607-2619.
- Belcher EH and Harriss EB (1957) Studies of plasma volume, red cell volume and total blood volume in young growing rats. *The Journal of physiology* **139**:64-78.
- Beltowski J, Rachanczyk J and Wlodarczyk M (2013) Thiazolidinedione-induced fluid retention: recent insights into the molecular mechanisms. *PPAR research* **2013**:628628.
- Berger J and Moller DE (2002) The mechanisms of action of PPARs. *Annual review of medicine* **53**:409-435.
- Berger JP, Petro AE, Macnaul KL, Kelly LJ, Zhang BB, Richards K, Elbrecht A, Johnson BA, Zhou G, Doebber TW, Biswas C, Parikh M, Sharma N, Tanen MR, Thompson GM, Ventre J, Adams AD, Mosley R, Surwit RS and Moller DE (2003) Distinct properties and advantages of a novel peroxisome proliferator-activated protein [gamma] selective modulator. *Molecular endocrinology* **17**:662-676.
- Buchanan TA, Meehan WP, Jeng YY, Yang D, Chan TM, Nadler JL, Scott S, Rude RK and Hsueh WA (1995) Blood pressure lowering by pioglitazone. Evidence for a direct vascular effect. *The Journal of clinical investigation* **96**:354-360.

JPET #250985

Campbell MJ, Carlberg C and Koeffler HP (2008) A Role for the PPARgamma in Cancer Therapy. *PPAR research* **2008**:314974.

Chen L, Yang B, McNulty JA, Clifton LG, Binz JG, Grimes AM, Strum JC, Harrington WW, Chen Z, Balon TW, Stimpson SA and Brown KK (2005) GI262570, a peroxisome proliferator-activated receptor {gamma} agonist, changes electrolytes and water reabsorption from the distal nephron in rats. *The Journal of pharmacology and experimental therapeutics* **312**:718-725.

Constien R, Forde A, Liliensiek B, Grone HJ, Nawroth P, Hammerling G and Arnold B (2001) Characterization of a novel EGFP reporter mouse to monitor Cre recombination as demonstrated by a Tie2 Cre mouse line. *Genesis* **30**:36-44.

de Souza CJ, Eckhardt M, Gagen K, Dong M, Chen W, Laurent D and Burkey BF (2001) Effects of pioglitazone on adipose tissue remodeling within the setting of obesity and insulin resistance. *Diabetes* **50**:1863-1871.

Delea TE, Edelsberg JS, Hagiwara M, Oster G and Phillips LS (2003) Use of thiazolidinediones and risk of heart failure in people with type 2 diabetes: a retrospective cohort study. *Diabetes care* **26**:2983-2989.

Food\_and\_Drug\_Administration US (2013) FDA Drug Safety Communication: FDA requires removal of some prescribing and dispensing restrictions for rosiglitazone-containing diabetes medicines. <http://www.fda.gov/Drugs/DrugSafety/ucm376389.html>.

JPET #250985

Food\_and\_Drug\_Administration US (2015) FDA Drug Safety Communication: FDA eliminates the Risk Evaluation and Mitigation Strategy (REMS) for rosiglitazone-containing diabetes medicines. <http://www.fda.gov/Drugs/DrugSafety/ucm476466.html>.

Gale EA (2001) Lessons from the glitazones: a story of drug development. *Lancet* **357**:1870-1875.

Gensch C, Clever YP, Werner C, Hanhoun M, Bohm M and Laufs U (2007) The PPAR-gamma agonist pioglitazone increases neoangiogenesis and prevents apoptosis of endothelial progenitor cells. *Atherosclerosis* **192**:67-74.

Ghazzi MN, Perez JE, Antonucci TK, Driscoll JH, Huang SM, Faja BW and Whitcomb RW (1997) Cardiac and glycemic benefits of troglitazone treatment in NIDDM. The Troglitazone Study Group. *Diabetes* **46**:433-439.

Guan Y, Hao C, Cha DR, Rao R, Lu W, Kohan DE, Magnuson MA, Redha R, Zhang Y and Breyer MD (2005) Thiazolidinediones expand body fluid volume through PPARgamma stimulation of ENaC-mediated renal salt absorption. *Nature medicine* **11**:861-866.

Haffner SM, Greenberg AS, Weston WM, Chen H, Williams K and Freed MI (2002) Effect of rosiglitazone treatment on nontraditional markers of cardiovascular disease in patients with type 2 diabetes mellitus. *Circulation* **106**:679-684.

Hansen L, Ekstrom CT, Tabanera YPR, Anant M, Wassermann K and Reinhardt RR (2006) The Pro12Ala variant of the PPARG gene is a risk factor for peroxisome proliferator-activated

*JPET* #250985

receptor-gamma/alpha agonist-induced edema in type 2 diabetic patients. *The Journal of clinical endocrinology and metabolism* **91**:3446-3450.

Hollenberg NK (2003) Considerations for management of fluid dynamic issues associated with thiazolidinediones. *The American journal of medicine* **115 Suppl 8A**:111S-115S.

Home PD, Pocock SJ, Beck-Nielsen H, Curtis PS, Gomis R, Hanefeld M, Jones NP, Komajda M, McMurray JJ and Team RS (2009) Rosiglitazone evaluated for cardiovascular outcomes in oral agent combination therapy for type 2 diabetes (RECORD): a multicentre, randomised, open-label trial. *Lancet* **373**:2125-2135.

Hosokawa M, Tsukada H, Fukuda K, Oya M, Onomura M, Nakamura H, Kodama M, Yamada Y and Seino Y (1999) Troglitazone inhibits bicarbonate secretion in rat and human duodenum. *The Journal of pharmacology and experimental therapeutics* **290**:1080-1084.

Iwasaki K, Zhang R, Perhonen MA, Zuckerman JH and Levine BD (2004) Reduced baroreflex control of heart period after bed rest is normalized by acute plasma volume restoration. *American journal of physiology Regulatory, integrative and comparative physiology* **287**:R1256-1262.

Kanda T, Brown JD, Orasanu G, Vogel S, Gonzalez FJ, Sartoretto J, Michel T and Plutzky J (2009) PPARgamma in the endothelium regulates metabolic responses to high-fat diet in mice. *The Journal of clinical investigation* **119**:110-124.

Kawasaki J, Hirano K, Nishimura J, Fujishima M and Kanaide H (1998) Mechanisms of vasorelaxation induced by troglitazone, a novel antidiabetic drug, in the porcine coronary artery. *Circulation* **98**:2446-2452.

JPET #250985

Keller H, Dreyer C, Medin J, Mahfoudi A, Ozato K and Wahli W (1993) Fatty acids and retinoids control lipid metabolism through activation of peroxisome proliferator-activated receptor-retinoid X receptor heterodimers. *Proceedings of the National Academy of Sciences of the United States of America* **90**:2160-2164.

Kisanuki YY, Hammer RE, Miyazaki J, Williams SC, Richardson JA and Yanagisawa M (2001) Tie2-Cre transgenic mice: a new model for endothelial cell-lineage analysis in vivo. *Developmental biology* **230**:230-242.

Kliewer SA, Umesono K, Noonan DJ, Heyman RA and Evans RM (1992) Convergence of 9-cis retinoic acid and peroxisome proliferator signalling pathways through heterodimer formation of their receptors. *Nature* **358**:771-774.

Kliewer SA, Xu HE, Lambert MH and Willson TM (2001) Peroxisome proliferator-activated receptors: from genes to physiology. *Recent progress in hormone research* **56**:239-263.

Kobayashi M, Inoue K, Warabi E, Minami T and Kodama T (2005) A simple method of isolating mouse aortic endothelial cells. *Journal of atherosclerosis and thrombosis* **12**:138-142.

Kotchen TA, Zhang HY, Reddy S and Hoffmann RG (1996) Effect of pioglitazone on vascular reactivity in vivo and in vitro. *The American journal of physiology* **270**:R660-666.

Kung J and Henry RR (2012) Thiazolidinedione safety. *Expert opinion on drug safety* **11**:565-579.

JPET #250985

Liu LF, Purushotham A, Wendel AA and Belury MA (2007) Combined effects of rosiglitazone and conjugated linoleic acid on adiposity, insulin sensitivity, and hepatic steatosis in high-fat-fed mice. *American journal of physiology Gastrointestinal and liver physiology* **292**:G1671-1682.

Marx N, Bourcier T, Sukhova GK, Libby P and Plutzky J (1999) PPARgamma activation in human endothelial cells increases plasminogen activator inhibitor type-1 expression: PPARgamma as a potential mediator in vascular disease. *Arteriosclerosis, thrombosis, and vascular biology* **19**:546-551.

Mehta D and Malik AB (2006) Signaling mechanisms regulating endothelial permeability. *Physiological reviews* **86**:279-367.

Merrill DC and Cowley AW, Jr. (1987) Chronic effects of vasopressin on fluid volume distribution in conscious dogs. *The American journal of physiology* **252**:F26-31.

Nesto RW, Bell D, Bonow RO, Fonseca V, Grundy SM, Horton ES, Le Winter M, Porte D, Semenkovich CF, Smith S, Young LH and Kahn R (2004) Thiazolidinedione use, fluid retention, and congestive heart failure: a consensus statement from the American Heart Association and American Diabetes Association. *Diabetes care* **27**:256-263.

Nicol CJ, Adachi M, Akiyama TE and Gonzalez FJ (2005) PPARgamma in endothelial cells influences high fat diet-induced hypertension. *American journal of hypertension* **18**:549-556.

Nissen SE and Wolski K (2007) Effect of rosiglitazone on the risk of myocardial infarction and death from cardiovascular causes. *The New England journal of medicine* **356**:2457-2471.

JPET #250985

Ogihara T, Rakugi H, Ikegami H, Mikami H and Masuo K (1995) Enhancement of insulin sensitivity by troglitazone lowers blood pressure in diabetic hypertensives. *American journal of hypertension* **8**:316-320.

Okuno A, Tamemoto H, Tobe K, Ueki K, Mori Y, Iwamoto K, Umesono K, Akanuma Y, Fujiwara T, Horikoshi H, Yazaki Y and Kadowaki T (1998) Troglitazone increases the number of small adipocytes without the change of white adipose tissue mass in obese Zucker rats. *The Journal of clinical investigation* **101**:1354-1361.

Parulkar AA, Pendergrass ML, Granda-Ayala R, Lee TR and Fonseca VA (2001) Nonhypoglycemic effects of thiazolidinediones. *Annals of internal medicine* **134**:61-71.

Pavlov TS, Levchenko V, Karpushev AV, Vandewalle A and Staruschenko A (2009) Peroxisome proliferator-activated receptor gamma antagonists decrease Na<sup>+</sup> transport via the epithelial Na<sup>+</sup> channel. *Molecular pharmacology* **76**:1333-1340.

Pershadsingh HA, Szollosi J, Benson S, Hyun WC, Feuerstein BG and Kurtz TW (1993) Effects of ciglitazone on blood pressure and intracellular calcium metabolism. *Hypertension* **21**:1020-1023.

Quirk PC, Ward LC, Thomas BJ, Holt TL, Shepherd RW and Cornish BH (1997) Evaluation of bioelectrical impedance for prospective nutritional assessment in cystic fibrosis. *Nutrition* **13**:412-416.

JPET #250985

Rao F, Yang RQ, Chen XS, Xu JS, Fu HM, Su H and Wang L (2014) PPARgamma Ligands Decrease Hydrostatic Pressure-Induced Platelet Aggregation and Proinflammatory Activity. *PloS one* **9**:e89654.

Rennings AJ, Smits P, Stewart MW and Tack CJ (2006) Fluid retention and vascular effects of rosiglitazone in obese, insulin-resistant, nondiabetic subjects. *Diabetes care* **29**:581-587.

Ricote M and Glass CK (2007) PPARs and molecular mechanisms of transrepression. *Biochimica et biophysica acta* **1771**:926-935.

Romer LH, Birukov KG and Garcia JG (2006) Focal adhesions: paradigm for a signaling nexus. *Circulation research* **98**:606-616.

Ross MG and Idah R (2004) Correlation of maternal plasma volume and composition with amniotic fluid index in normal human pregnancy. *The journal of maternal-fetal & neonatal medicine : the official journal of the European Association of Perinatal Medicine, the Federation of Asia and Oceania Perinatal Societies, the International Society of Perinatal Obstet* **15**:104-108.

Schmidt TT, Tauseef M, Yue L, Bonini MG, Gothert J, Shen TL, Guan JL, Predescu S, Sadikot R and Mehta D (2013) Conditional deletion of FAK in mice endothelium disrupts lung vascular barrier function due to destabilization of RhoA and Rac1 activities. *American journal of physiology Lung cellular and molecular physiology* **305**:L291-300.



JPET #250985

Song J, Walsh MF, Igwe R, Ram JL, Barazi M, Dominguez LJ and Sowers JR (1997) Troglitazone reduces contraction by inhibition of vascular smooth muscle cell Ca<sup>2+</sup> currents and not endothelial nitric oxide production. *Diabetes* **46**:659-664.

Spiegelman BM, Hu E, Kim JB and Brun R (1997) PPAR gamma and the control of adipogenesis. *Biochimie* **79**:111-112.

Starner CI, Schafer JA, Heaton AH and Gleason PP (2008) Rosiglitazone and pioglitazone utilization from January 2007 through May 2008 associated with five risk-warning events. *Journal of managed care pharmacy : JMCP* **14**:523-531.

Sugawara A, Takeuchi K, Uruno A, Ikeda Y, Arima S, Kudo M, Sato K, Taniyama Y and Ito S (2001) Transcriptional suppression of type 1 angiotensin II receptor gene expression by peroxisome proliferator-activated receptor-gamma in vascular smooth muscle cells. *Endocrinology* **142**:3125-3134.

Sugawara A, Uruno A, Matsuda K, Saito-Ito T, Funato T, Saito-Hakoda A, Kudo M and Ito S (2012) Effects of PPARgamma agonists against vascular and renal dysfunction. *Current molecular pharmacology* **5**:248-254.

Tontonoz P, Hu E, Graves RA, Budavari AI and Spiegelman BM (1994) mPPAR gamma 2: tissue-specific regulator of an adipocyte enhancer. *Genes & development* **8**:1224-1234.

Uruno A, Matsuda K, Noguchi N, Yoshikawa T, Kudo M, Satoh F, Rainey WE, Hui XG, Akahira J, Nakamura Y, Sasano H, Okamoto H, Ito S and Sugawara A (2011) Peroxisome

JPET #250985

proliferator-activated receptor- $\gamma$  suppresses CYP11B2 expression and aldosterone production. *Journal of molecular endocrinology* **46**:37-49.

Vallon V, Hummler E, Rieg T, Pochynyuk O, Bugaj V, Schroth J, Dechenes G, Rossier B, Cunard R and Stockand J (2009) Thiazolidinedione-induced fluid retention is independent of collecting duct  $\alpha$ ENaC activity. *Journal of the American Society of Nephrology : JASN* **20**:721-729.

Wagner MC, Yeligar SM, Brown LA and Michael Hart C (2012) PPAR $\gamma$  ligands regulate NADPH oxidase, eNOS, and barrier function in the lung following chronic alcohol ingestion. *Alcoholism, clinical and experimental research* **36**:197-206.

Wahli W, Braissant O and Desvergne B (1995) Peroxisome proliferator activated receptors: transcriptional regulators of adipogenesis, lipid metabolism and more. *Chemistry & biology* **2**:261-266.

Walker AB, Chattington PD, Buckingham RE and Williams G (1999) The thiazolidinedione rosiglitazone (BRL-49653) lowers blood pressure and protects against impairment of endothelial function in Zucker fatty rats. *Diabetes* **48**:1448-1453.

Wang LH, Yang XY, Zhang X, Huang J, Hou J, Li J, Xiong H, Mihalic K, Zhu H, Xiao W and Farrar WL (2004) Transcriptional inactivation of STAT3 by PPAR $\gamma$  suppresses IL-6-responsive multiple myeloma cells. *Immunity* **20**:205-218.

Willson TM, Lambert MH and Kliewer SA (2001) Peroxisome proliferator-activated receptor  $\gamma$  and metabolic disease. *Annual review of biochemistry* **70**:341-367.

*JPET* #250985

Yki-Jarvinen H (2004) Thiazolidinediones. *The New England journal of medicine* **351**:1106-1118.

Yoshimoto T, Naruse M, Nishikawa M, Naruse K, Tanabe A, Seki T, Imaki T, Demura R, Aikawa E and Demura H (1997) Antihypertensive and vasculo- and renoprotective effects of pioglitazone in genetically obese diabetic rats. *The American journal of physiology* **272**:E989-996.

Zhang H, Zhang A, Kohan DE, Nelson RD, Gonzalez FJ and Yang T (2005) Collecting duct-specific deletion of peroxisome proliferator-activated receptor gamma blocks thiazolidinedione-induced fluid retention. *Proceedings of the National Academy of Sciences of the United States of America* **102**:9406-9411.

*JPET #250985*

## FOOTNOTES

This work was supported by funding from Merck Research Laboratories to TEA, LAM, NS, EIZ, HL, JWW, CHC and JPB, and the Canadian Breast Cancer Foundation, Ontario Chapter [#369649] to CJBN. This research was supported [in part] by the Intramural Research Program of the National Institutes of Health [National Cancer Institute]. The funders had no role in study design, data collection and analysis, decision to publish, or preparation of the manuscript.

Reprint requests should be directed to CJBN, Queen's University Cancer Research Institute, 10 Stuart St., Rm 317, Kingston, Ontario, Canada K7L 3N6. Email: [nicolc@queensu.ca](mailto:nicolc@queensu.ca)

TEA and GESG contributed equally to this work

This article was prepared while TEA was employed at Merck & Co. The opinions expressed in this article are the author's own and do not reflect the view of the Food and Drug Administration, the Department of Health and Human Services, or the United States government.

JPET #250985

## FIGURE LEGENDS

### **Figure 1. High Fat Diet Effect on Body Mass Composition of *Pparg*<sup>ff</sup> and *Pparg*<sup>ΔEC</sup> mice.**

qNMR was performed on *Pparg*<sup>ff</sup> and *Pparg*<sup>ΔEC</sup> mice following 12 week treatment on HF diet.

Values are presented as a percent of total body weight.

### **Figure 2. Rosiglitazone Effects on Plasma Glucose and Insulin levels in *Pparg*<sup>ff</sup> and**

***Pparg*<sup>ΔEC</sup> mice.** Plasma glucose (A) and insulin (B) values were determined in *Pparg*<sup>ff</sup> and

*Pparg*<sup>ΔEC</sup> mice prior to and following vehicle or rosiglitazone treatment for 14 days as described in the Methods. Values represent mean + SE. \*, significantly different compared to respective vehicle controls, p<0.05.

### **Figure 3. Histological analysis of epididymal white adipose tissue from *Pparg*<sup>ff</sup> and**

***Pparg*<sup>ΔEC</sup> mice.** FFPE samples from each treatment group were assessed as described in

Methods section. Panels A–vehicle-treated *Pparg*<sup>ff</sup> mice, B–rosiglitazone-treated *Pparg*<sup>ff</sup> mice, C- vehicle-treated *Pparg*<sup>ΔEC</sup> mice, and D- rosiglitazone-treated *Pparg*<sup>ΔEC</sup> mice. The bar in lower right of panel D is 50 microns long. Arrowheads in panels A, C and D indicate single red blood cells in normal capillary cut in cross section. Short arrows in panels A, C and D point to multiple red blood cells lined up in single file in normal capillary laying in the plane of the section. Long (concave) arrows in panel B point to abnormally large capillaries observed only in eWAT from rosiglitazone-treated *Pparg*<sup>ff</sup> mice.

### **Figure 4. Quantitation of enlarged capillaries in epididymal and inguinal white adipose**

**tissue.** A) epididymal and B) inguinal adipose tissue were fixed, dehydrated, paraffin embedded

JPET #250985

and stained with hematoxylin and eosin. Enlarged capillaries were from 10 widely separated locations of preserved adipocytes not large blood vessels, lymph nodes or connective tissue. \*, significantly different compared to respective vehicle controls,  $p < 0.05$ .

**Figure 5. Role of endothelial PPAR $\gamma$  expression on measures of rosiglitazone-mediated edema.** A) qNMR was performed on *Pparg*<sup>ff</sup> and *Pparg* <sup>$\Delta$ EC</sup> mice following vehicle or rosiglitazone treatment as described above. Values represent absolute fluid mass in milliliters. B) Extracellular fluid volume in *Pparg*<sup>ff</sup> and *Pparg* <sup>$\Delta$ EC</sup> mice following vehicle or rosiglitazone treatment as determined by bioimpedance measurements. C) Plasma volume in *Pparg*<sup>ff</sup> and *Pparg* <sup>$\Delta$ EC</sup> mice following vehicle or rosiglitazone treatment as determined by the Evan's blue assay. All values are reported as mean + SE. \*, significantly different compared to respective vehicle controls,  $p < 0.05$ .

**Figure 6. Tissue water content in vehicle- or rosiglitazone-treated *Pparg*<sup>ff</sup> and *Pparg* <sup>$\Delta$ EC</sup> mice.** Water content in epididymal, inguinal and retroperitoneal white adipose tissue and skeletal muscle in vehicle- or rosiglitazone-treated *Pparg*<sup>ff</sup> and *Pparg* <sup>$\Delta$ EC</sup> mice was assessed following tissue collection at necropsy. The difference between wet tissue weight and dry tissue weight following lyophilization (reflecting absolute water weight) was normalized to wet tissue weight prior to lyophilization. All values are reported as mean + SE. \*, significantly different compared to respective vehicle controls,  $p < 0.05$ .

**Figure 7. Endothelial expression changes in vehicle- or rosiglitazone-treated *Pparg*<sup>ff</sup> and *Pparg* <sup>$\Delta$ EC</sup> mice.** A-B) Analysis of *Pparg* and *Fak* mRNAs within isolated lung ECs from (n=3)

JPET #250985

untreated *Pparg*<sup>ff</sup> and *Pparg*<sup>ΔEC</sup> mice. All values are calculated relative to the internal control *Gapdh* mRNA, and reported as a mean percentage ±SD of mRNA expression in *Pparg*<sup>ff</sup> mice. C-E) Immunofluorescent evaluation of VE-cadherin in EC junctions from lung samples of (n=3) *Pparg*<sup>ff</sup> and *Pparg*<sup>ΔEC</sup> mice. Samples were stained with DAPI (blue), PECAM (green) and VE-cadherin (red). C) Representative image from *Pparg*<sup>ff</sup> lung sample. D) Representative image from *Pparg*<sup>ΔEC</sup> lung sample. E) Integrated intensity of VE-cadherin expression in EC junctions of *Pparg*<sup>ff</sup> and *Pparg*<sup>ΔEC</sup> mice. \*, significantly different compared to controls, p<0.05.

**Figure 8. Summary model of PPARγ-dependent edema mechanism.** A) ROSI-mediated activation of PPARγ signaling in ECs suppresses FAK, leading to direct or indirect decreases in VE-Cadherin expression and EC adherens junctions, allowing for increased edema. B) Loss of PPARγ expression/signaling abrogates FAK repression and enhances VE-cadherin expression and adherens junctions between ECs, thereby minimizing edema.

**Fig 1**

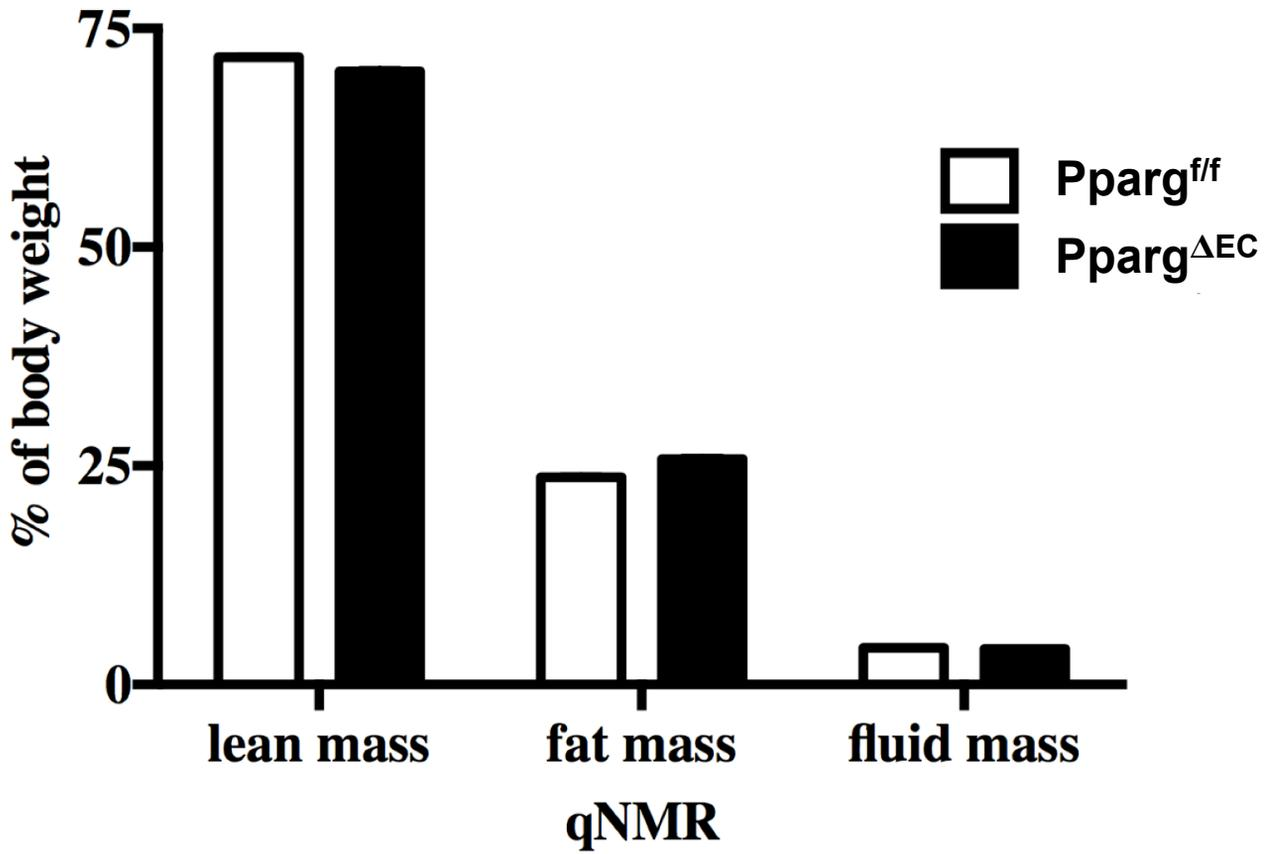




**Fig 2**

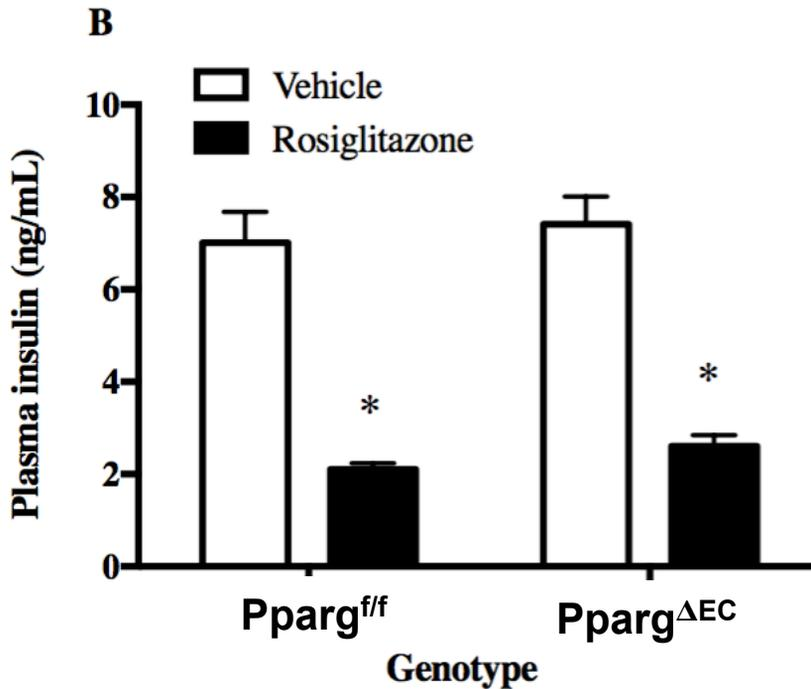
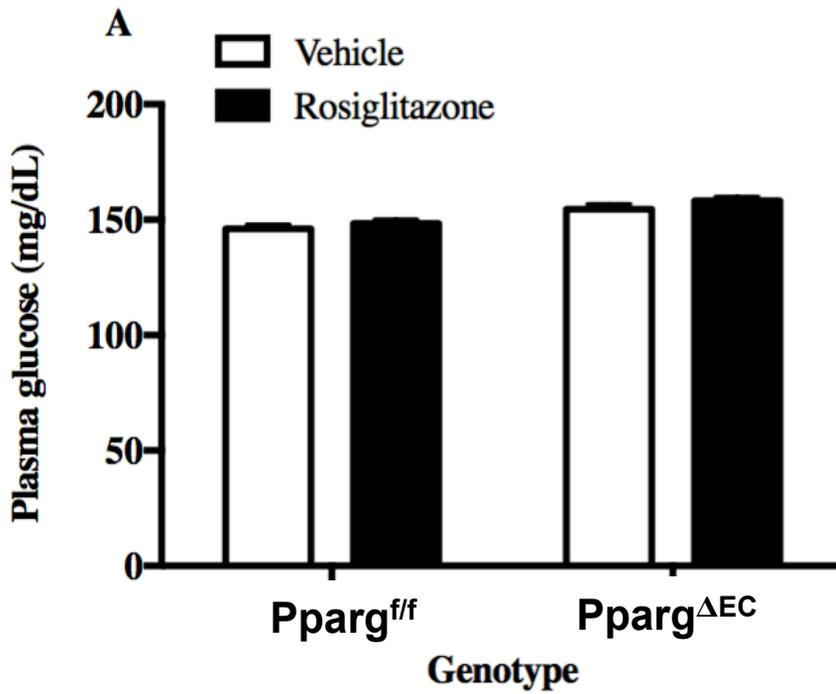


**Fig 3**

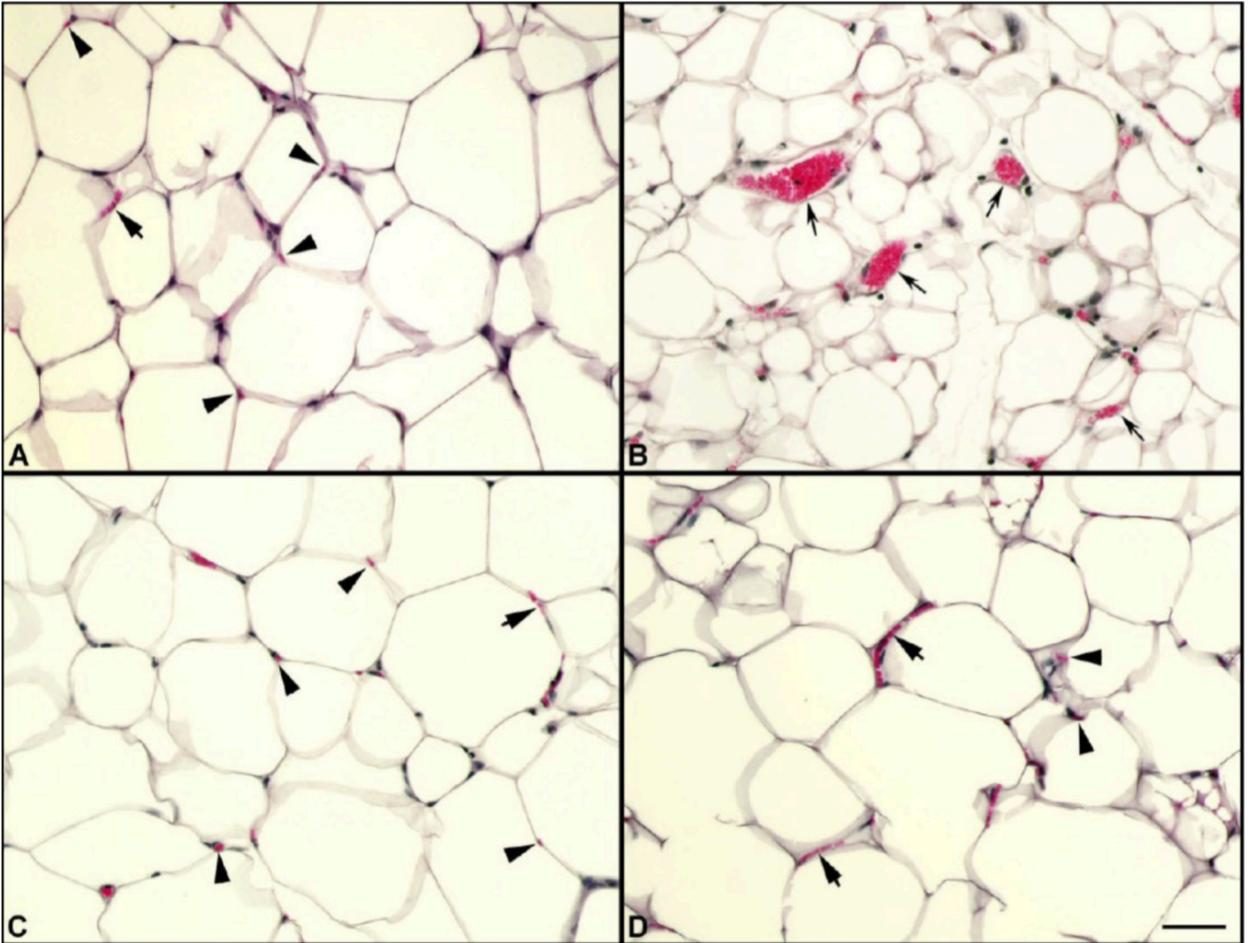


**Fig 4**  
**eWAT**

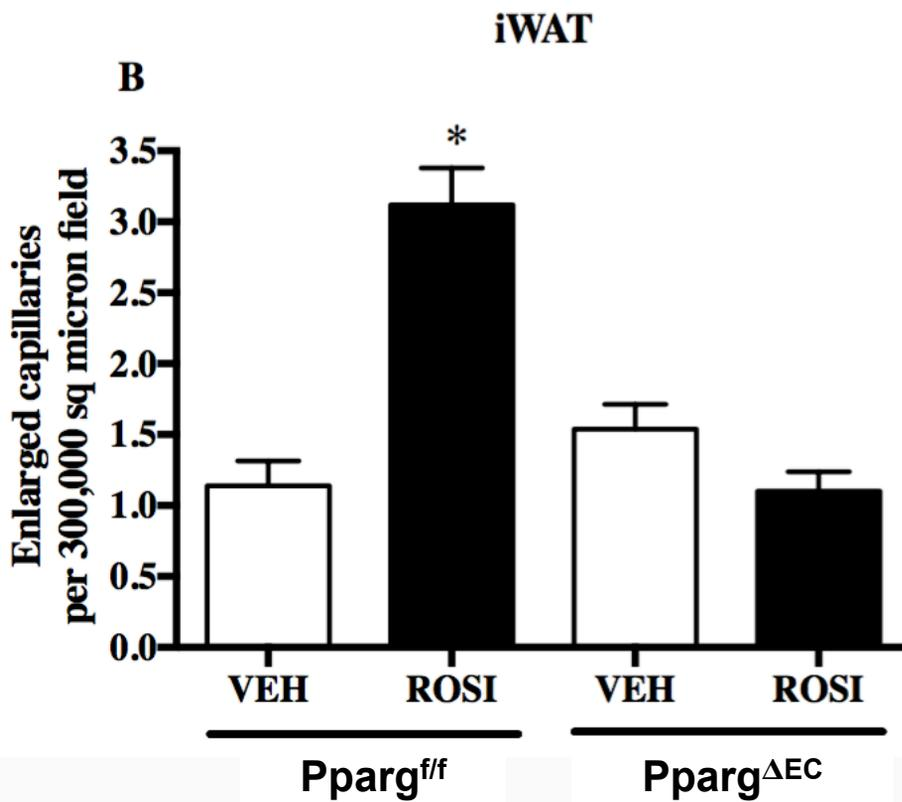
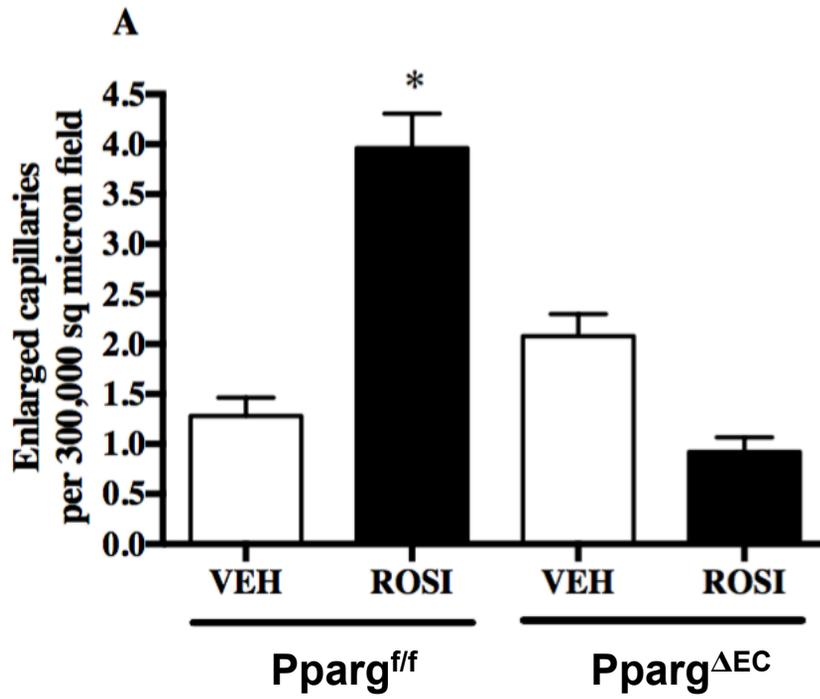
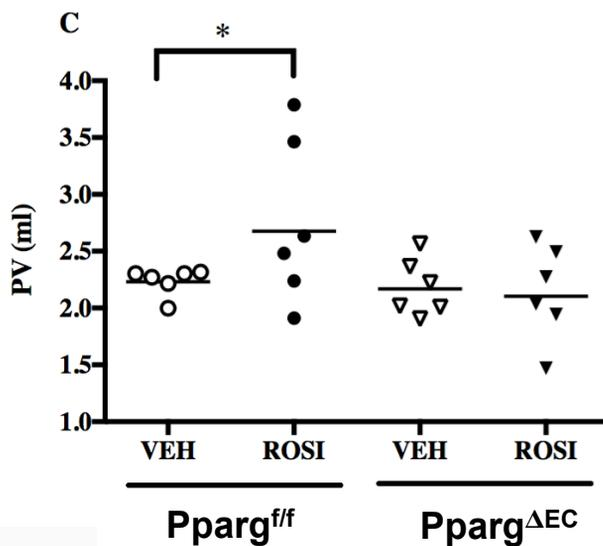
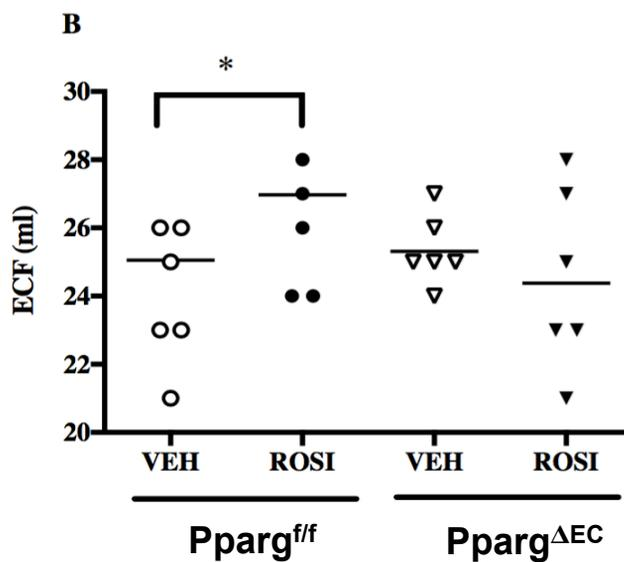
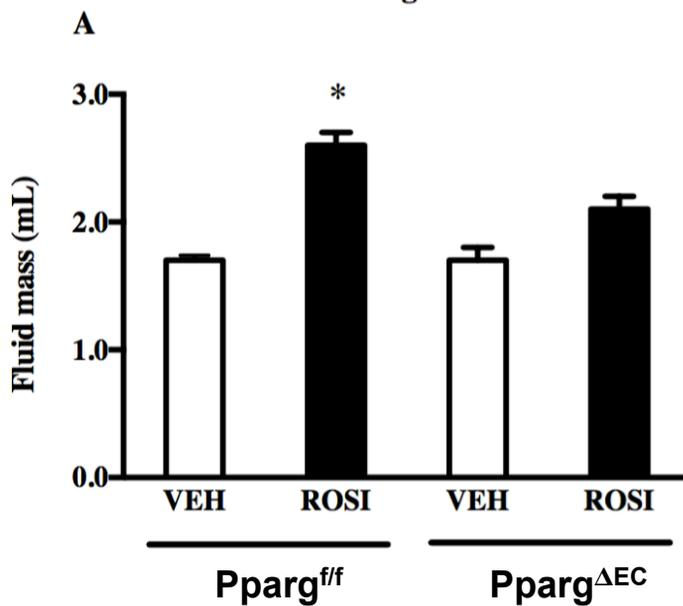


Fig 5



**Fig 6**

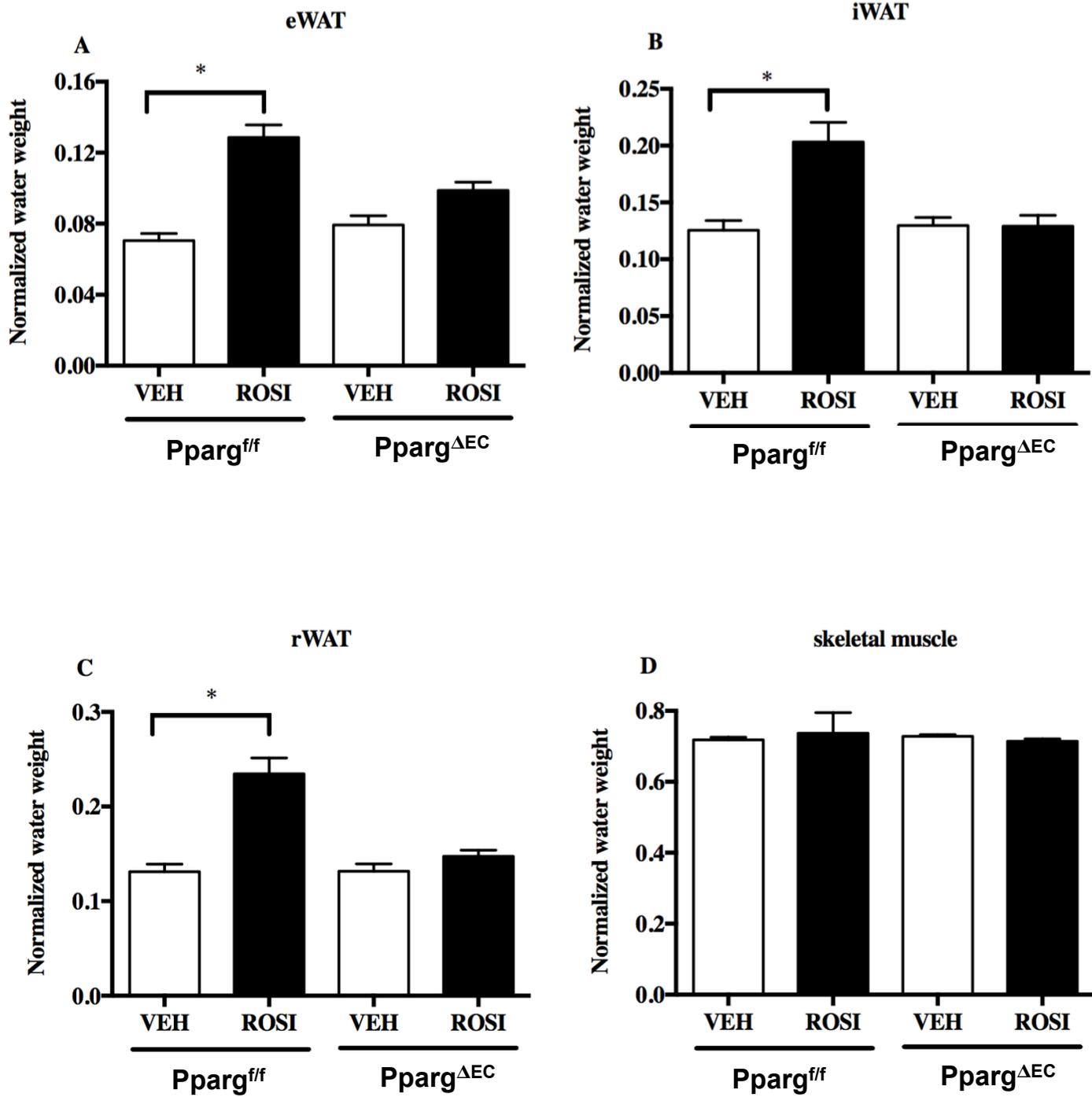
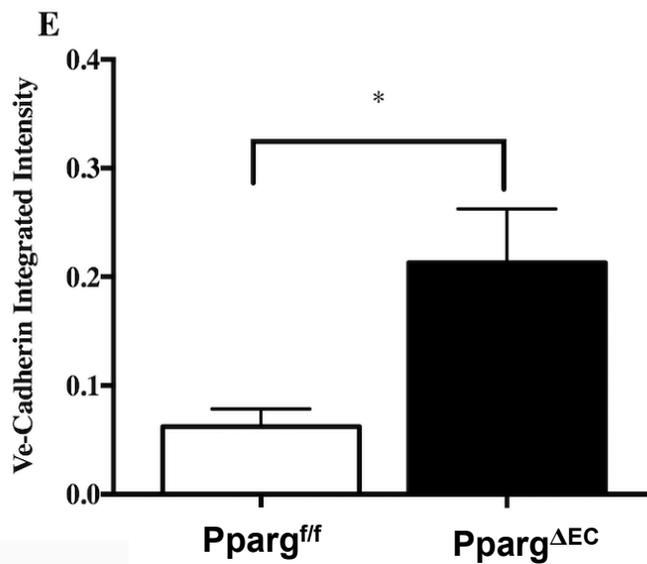
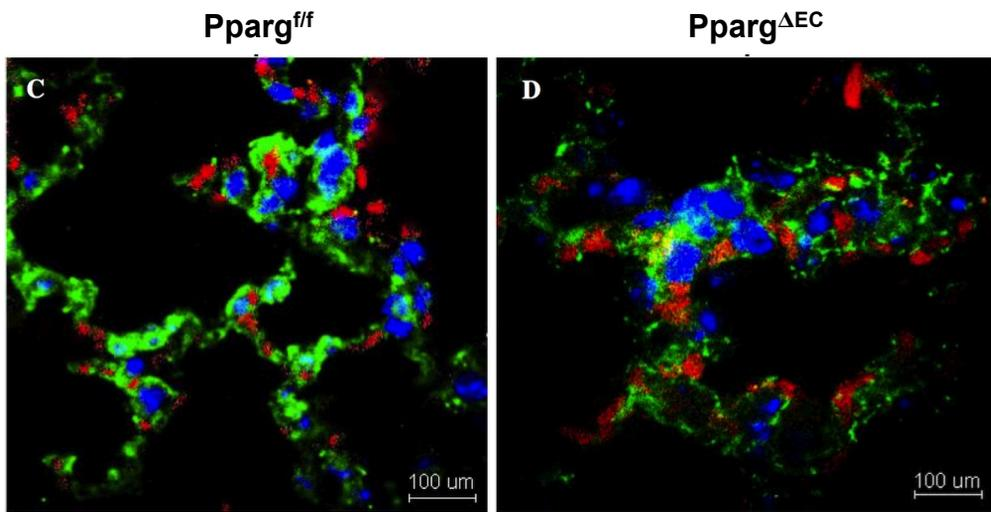
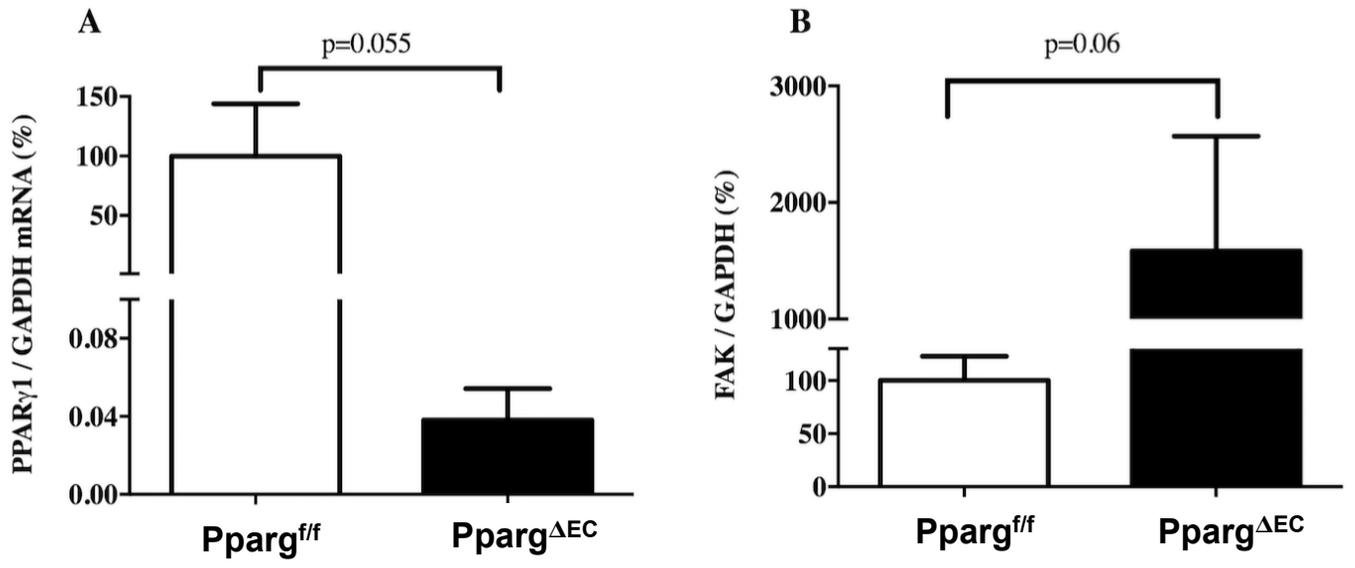


Fig 7



**Fig 8**

